## Atom Indonesia

# Neutronic Design Modification of Passive Compact-Molten Salt Reactor

## R. A. P. Dwijayanto[1*], A. W. Harto[2]

[1] *Research Centre for Nuclear Reactor Technology, Research Organisation for Nuclear Energy, National Research and Innovation Agency, BJ Habibie Science and Technology Centre, Building No. 80, South Tangerang 15314, Indonesia*
[2] *Department of Nuclear Engineering and Physics Engineering, Faculty of Engineering, Universitas Gadjah Mada, Jl. Grafika No. 2, Yogyakarta 55281, Indonesia*

**A R T I C L E   I N F O**

**A B S T R A C T**

Passive compact molten salt reactor (PCMSR) is a design concept of a molten salt reactor (MSR) currently under development in Universitas Gadjah Mada, Indonesia. It is designed as a thermal breeder reactor using thorium fuel cycle. However, our previous study shows that the original PCMSR design was incorrectly modelled, primarily overestimating its thorium breeding capability. To improve PCMSR neutronic design, we modified the core configuration by the addition of radial fuel channel layers previously nonexistent in original PCMSR core design in various configurations. Neutronic parameters of modified PCMSR geometries in the beginning of life (BOL) were simulated using MCNP6.2 radiation transport code with ENDF/B-VII.0 library. All variations of fuel layer addition show improvement in both temperature coefficient of reactivity (TCR) and breeding ratio (BR), with TCR values became more negative and BR values are larger than unity, ensuring proper breeding capability. Configuration Inner Core-Outer Blanket (IC-OB) achieves the largest BR and lowest doubling time (DT), whilst its TCR is an improvement from the original design. Therefore, IC-OB fuel layer configuration can be applied to redesign the original PCMSR and used in various design optimization scenarios.

## INTRODUCTION

The development of molten salt reactor (MSR) is geared towards both converter and breeder reactors. Whilst the former is easier to achieve due to less stringent requirements, fuel breeding in MSR is comparably more attractive than reactor breeding using solid-fueled reactors [1,2]. The key advantage is its molten salt fuel, which allows fuel reprocessing to be performed online, i.e., without shutting down the reactor. Fission products (FPs) and even transuranic (TRU) elements can be removed from the fuel whilst the reactor is operating, maintaining excellent neutron economy within the core. Apart from that, molten salt is highly resistant to radiation damage; this allows the nuclear fuel to remain indefinitely inside the core, safe from solubility limit of the salt compound [3].

Thus, thermal breeding in MSR is an attractive option for sustainable nuclear fuel cycle.

This, however, limits the fuel cycle to thorium fuel cycle. U-233 bred from Th-232 is the only fissile nuclide capable of providing sufficient excess neutron to breed larger amount of fissile fuel than its consumption in thermal neutron spectrum. Online fuel reprocessing also allows Pa-233, the precursor of U-233, to be removed from the core and let decay into U-233 to avoid parasitic neutron capture from its decent capture cross section and comparably longer half-life (27 days) compared to Np-239 (2.3 days), the latter is Pu-239 precursor in uranium fuel cycle. This is why MSRs are generally associated with thorium fuel cycle, such as the progenitor of thermal breeder MSR, the Molten Salt Breeder Reactor (MSBR), developed by Oak Ridge National Laboratory (ORNL) [4-6].

The MSBR was designed as a one fluid thermal breeder MSR with 2,250 MWt of thermal power and operational temperature of 700 °C. The core is moderated by graphite with square fuel channel lattice pierced through the moderator [3,5,6]. MSBR fuel salt consists of eutectic Flibe ($^7$LiF-BeF$_2$) carrier salt where ThF$_4$ and $^{233}$UF$_4$

are dissolved within. This fuel composition set as the typical fuel salt preference in later thermal breeder MSR designs. With reprocessing rate of 4.6 m$^3$ fuel salt/day, the MSBR can achieve breeding ratio around 1.06 with doubling time of 21 years [4], though later studies stated that its doubling time may be longer at 31 years [7] or even shorter at 17.4 years [8].

After MSBR development was abruptly stopped in late 1970s, Japan developed a 450 MWt break even MSR called MSR-FUJI [9,10]. It was designed to breed only enough U-233 for its own consumption, omitting online fuel reprocessing, save for gaseous FP removal. Its low power density and three zones core was applied to flatten the neutron flux throughout the core, so that the graphite moderator can last up to 30 years. MSR-FUJI concept was accompanied by an accelerator-driven system (ADS) to externally generate U-233 as its startup fuel [11,12].

In the past decade, China started their national strategic project called "Future Advanced Nuclear Energy-Thorium-based Molten Salt Reactor System (TMSR)" [7] which encompasses various types of MSRs, such as fast-spectrum MSR [13,14], fluoride salt-cooled high temperature reactor (FHR) [15,16], and most recently Single fluid Double zone-Thorium Molten Salt Reactor (SD-TMSR) [17,18]. SD-TMSR is a 2,250 MWt thermal breeder MSR whose design was inspired by the MSBR and French Molten Salt Fast Reactor (MSFR). A full-fledged thermal breeder MSR, it employs online fuel reprocessing able to remove FPs, actinides, and TRUs through helium sparging, fluorination, and reductive extraction. The optimized core design can achieve doubling time at around 16 years [17], compared to MSBR at ± 21 years [4].

In Indonesia, development of thermal breeder MSR exists sparingly. A concept design called Passive Compact Molten Salt Reactor (PCMSR) [19] was originally developed in Department of Nuclear Engineering and Physics Engineering, Universitas Gadjah Mada. PCMSR was designed as a small modular thermal breeder MSR operating in much higher temperature than typical MSR (1,200 °C for PCMSR against 700 °C for typical MSR). The core was intended to generate 460 MWt of heat, fitted within a compact integral module consisting of reactor core, primary heat exchanger, secondary coolant, and tertiary coolant. Due to sparing development, however, PCMSR has no fixed core design [19-22]. Our previous study even concluded that the initial PCMSR core design was incapable of attaining thermal breeding, i.e., having neutronic deficiency [23].

As Indonesia possesses a fair amount of thorium potential [24], PCMSR may be suitable for optimal utilization of thorium; this could bring huge benefit for the nation. However, the neutronic deficiency must first be fixed so that the PCMSR can fulfil thermal breeding criterion with acceptable safety level. This research is the first attempt to modify the original PCMSR design in order to achieve those features, by applying a small tweak on the design. Further optimization with more detailed parameters and analyses will follow in the future.

## REACTOR DESCRIPTION

PCMSR refers more to a whole reactor module rather than the core design (see Fig. 1). This integral module consists of graphite-moderated reactor core and heat removal systems, in which the latter also work as post-shutdown cooling system. PCMSR reactor core can either be one-fluid or two-fluid core. However, most design studies of PCMSR were conducted using one-fluid core due to its design simplicity [19-22]. The initial design calculation was also one-fluid [19], in which neutronic economy was proven to be deficient by our recent study [23]. PCMSR core is moderated by graphite which can be replaced without shutting down the reactor. The core is placed on the top of primary shell-and-tube heat exchanger, which in turn surrounded by secondary molten salt to transfer the heat to tertiary molten salt. The latter then transfers the heat into the multi-reheat Brayton turbine. The secondary and tertiary salts also work as radiation shielding and passive heat removal system in the case of accident.
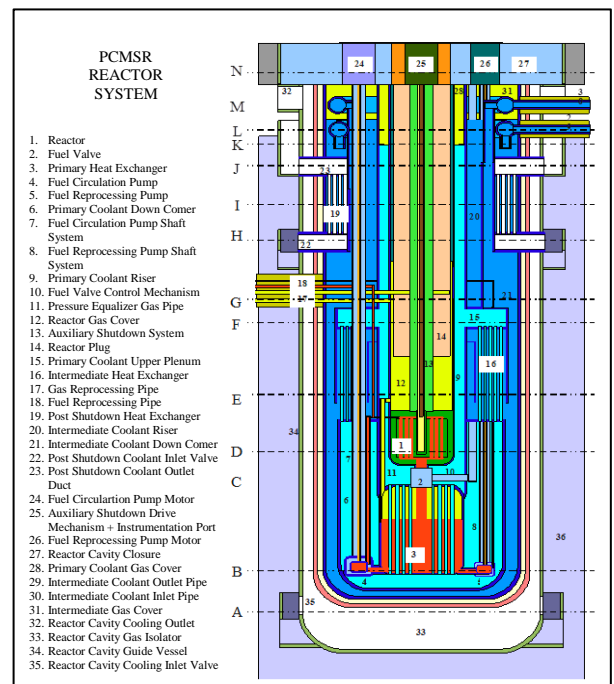


**Fig. 1.** PCMSR reactor system [20].

Operational parameters of PCMSR are summarized in Table 1. As a thermal breeder reactor, PCMSR operates in thorium fuel cycle. The fuel is a fluoride salt mixture, with primary composition of $^7$LiF-ThF$_4$-$^{233}$UF$_4$. The omission of BeF$_2$ from the fuel salt increases the salt's melting point to support its high operational temperature (1,200K, down from 1,473K in original design). LiF salt comprises 70% mole of the fuel salt, whilst the remaining 30% mole consists of ThF$_4$ and $^{233}$UF$_4$, whose composition is adjustable to maintain core criticality. This unusually large fuel salt inventory compensates for its small core size, along with high-density graphite moderator. Li-7 isotope is enriched to 100 % to minimize parasitic neutron capture from Li-6. It should be noted that 100 % enrichment is unrealistic in industrial scale, and this enrichment level was used to simulate the most ideal neutronic condition.

**Table 1.** PCMSR reactor parameters [23].

| Parameter | Value |
|---|---|
| Thermal power | 570 MWt |
| Active core diameter | 220 cm |
| Active core height | 220 cm |
| Graphite density | 2.2 g/cm$^3$ |
| Hastelloy thickness | 5 cm |
| Core channel radius | 4.5 cm |
| Blanket channel radius | 6.5 cm |
| Operational temperature | 1200K |
| Fuel type | Molten salt |
| Composition | 70%LiF-30%(HM)F$_4$ |
| Fuel density | 3.75 g/cm$^3$ |

The PCMSR core modelled in this study is a virtual one-and-half fluid core [1], as shown in Fig. 2. The singular molten salt stream is flown into the reactor core from the top and divided into two fuel channel zones in reactor core, referred as core and blanket zone. The former has smaller channel radius intended to enhance fission reaction, whilst the latter has larger channel radius to harden neutron spectrum so that thorium capture is improved. The heated fuel flows out of the core from the outlet at the bottom of the core, flowing into the primary heat exchanger.

The original PCMSR design has two separate radial graphite layers, the inner layer separates two core channel layers and the outer layer separates core channel from the blanket layer. Whilst the existence of these graphite layers does not necessarily compromise the moderator temperature feedback, it is the primary reason of low breeding ratio (BR) of the PCMSR core. Design modification will be applied in these layers, by inserting additional fuel layers in place of empty graphite layers.
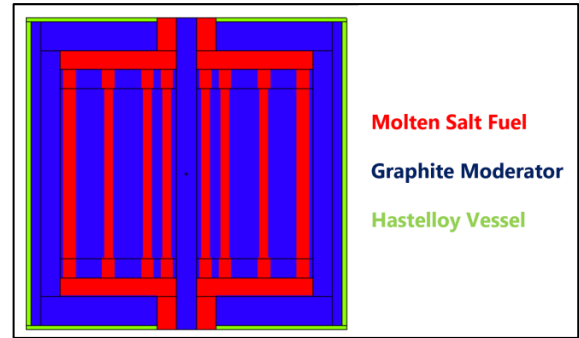


(a)
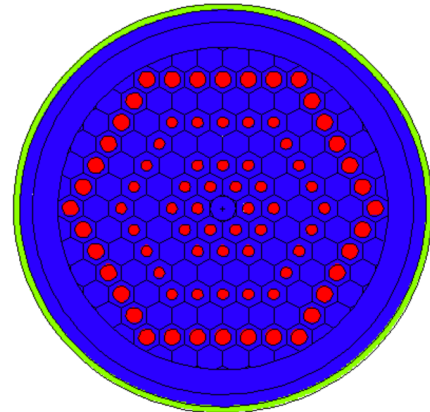


(b)

**Fig. 2.** MCNP model of original PCMSR core design (a) axial cross section, (b) radial cross section.

## METHODOLOGY

As previously mentioned in Section 2, design modifications were applied in the radial graphite layers exist in the original one-fluid PCMSR core design. As there are two graphite layers and two core zones, we can apply five different layer modifications, shown in Fig. 3. The variations are coded as follows.

a. Inner Core-Outer Core (IC-OC)
b. Inner Graphite-Outer Core (IG-OC)
c. Inner Core-Outer Blanket (IC-OB)
d. Inner Graphite-Outer Blanket (IG-OB)
e. Inner Core-Outer Graphite (IC-OG)

As the graphite layers flank a core channel layer, it makes no sense to put blanket channel in the inner graphite layer. Therefore, only Core and Graphite were considered to fill inner layer. The outer layer was filled with either Core, Blanket, or Graphite, the last of which only applied in one variation. Although theoretically two fuel layers can increase BR more significantly, one fuel layer addition was also considered anyway to evaluate whether such addition is sufficient, considering the fuel inventory in the active core. The volumes of fuel salt and graphite for each variation is summarized in Table 2.
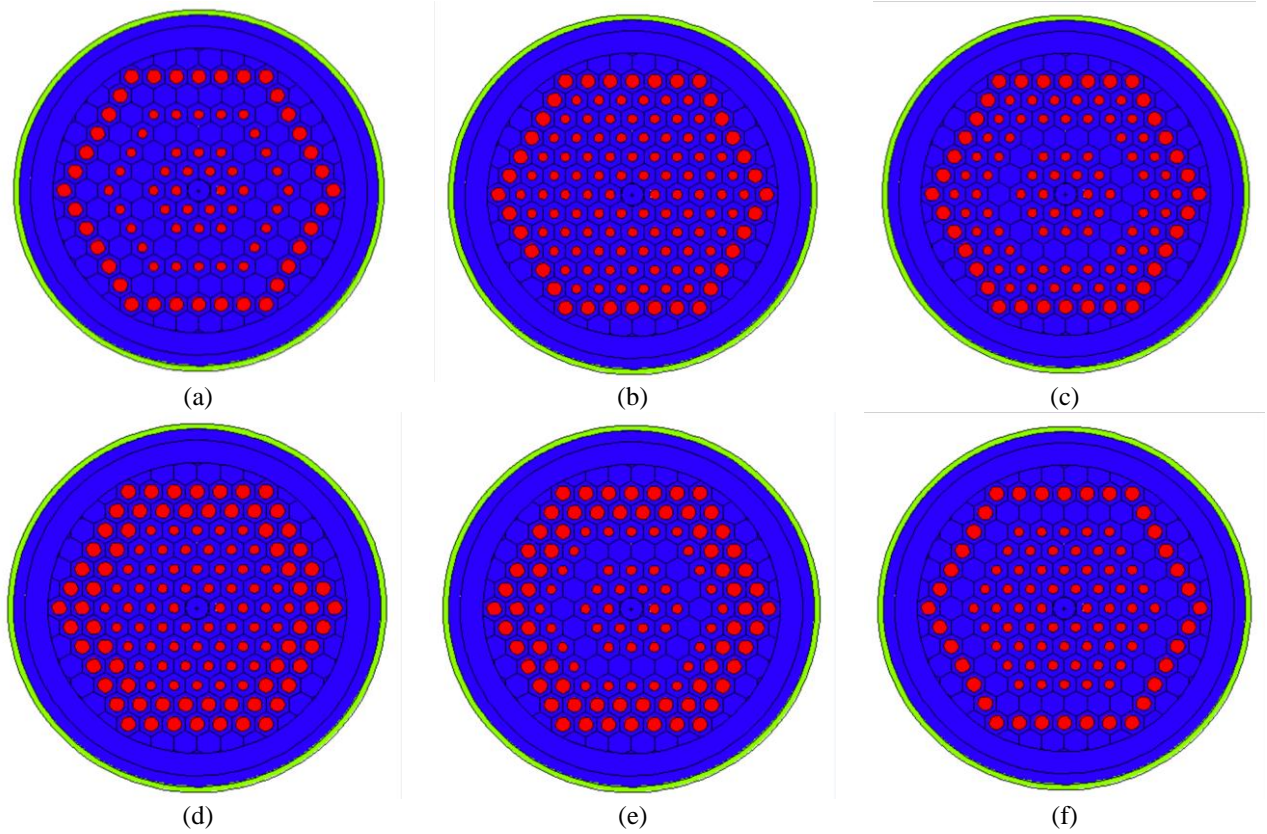
**Fig. 3.** PCMSR core modifications (a) Original design, (b) IC-OC, (c) IG-OC, (d) IC-OB, (e) IG-OB, (f) IC-OG.

**Table 2.** Fuel salt and graphite volume for each variation.

| Variation | Fuel Salt Volume (m³) | Graphite Volume (m³) |
|-----------|-----------------------|----------------------|
| Standard  | 1.27 | 10.41 |
| IC-OC     | 1.71 | 9.97 |
| IG-OC     | 1.51 | 10.17 |
| IC-OB     | 1.71 | 9.97 |
| IG-OB     | 1.51 | 10.17 |
| IC-OG     | 1.37 | 10.31 |

The objective of this design modification is to achieve a neutronically sufficient PCMSR core, which is characterized by a large BR, negative temperature coefficient of reactivity (TCR), short doubling time (DT), and reasonable fuel inventory. To obtain these values, a neutronic simulation was performed using the MCNP6.2 radiation transport code with the ENDF/B-VII.0 neutron cross-section library. MCNP is a well-established code for simulating the neutronic aspects of nuclear reactors and has been extensively used for various types of reactors [25-30]. Although MCNP may not be the most suitable simulation tool for MSR due to its decoupling from thermal-hydraulic calculations, it has nonetheless been used for simulating various MSR designs, such as MSBR [6,31,32], MSR-FUJI [9], TMSR-500 [33-35], and Integral Molten Salt Reactor (IMSR) [36], with good agreement to the reference. The original PCMSR design was also simulated with MCNP and found to be in good agreement with the Serpent-2 code [23].

The first parameter to be obtained was the effective multiplication factor ($k_{eff}$). The molar fractions of $ThF_4$ and $^{233}UF_4$ were adjusted to achieve $k_{eff}$ on the range of $1 \leq k_{eff} \leq 1 + \beta_{eff}$, to minimize excess reactivity below the prompt critical value. Close $k_{eff}$ value between each variation will provide a fairer analysis for the subsequent parameters. It must be noted, however, that due to the nature of circulating fuel of MSR, the $\beta_{eff}$ fraction in the core is reduced up to 50 % of the $\beta_{eff}$ value if the fuel is stationary [37-39]. This delayed precursor drift is beyond the scope of this study, and the $\beta_{eff}$ value obtained from criticality calculation was used as standard.

The second is TCR, in MSR it is described in Eq. (1) [7].

$$\frac{dk}{dT}\bigg)_{total} = \frac{dk}{dT}\bigg)_{salt\ density} + \frac{dk}{dT}\bigg)_{Doppler} + \frac{dk}{dT}\bigg)_{moderator} \qquad (1)$$

Doppler coefficient (DC) was obtained by decreasing fuel salt temperature to 900K whilst other components remain at constant temperature. Salt

density coefficient (SDC) was obtained by increasing fuel density to the density at 900K, and moderator temperature coefficient (MTC) was calculated by decreasing the graphite temperature to 900K and thermal scattering library s($\alpha$,$\beta$) to 1,000K [40], due to the absence of s($\alpha$,$\beta$) at 900K. As noted in Eq. 1, TCR is the sum of the aforementioned coefficients.

Meanwhile, BR is calculated at the beginning of life (BOL) only, due to MCNP6.2 does not possess the feature to simulate online reprocessing capability inherent to MSR. Future design optimization must consider online reprocessing using proper simulation tool in order to show a more comprehensive analysis on PCMSR neutronic behavior throughout its operational lifetime. BR values were calculated from reaction rate of fertile and fissile nuclides using Eq. (2).

$$BR = \frac{R_c(^{232}_{90}Th)}{R_A(^{233}_{92}U)} \qquad (2)$$

where $R_c$ is the capture reaction rate of Th-232 and $R_A$ is the absorption reaction rate of U-233.

DT typically refers to the time required to accumulate enough fissile to start an identical reactor. Accurate DT calculation must involve burnup calculation with online reprocessing system. Since MCNP code cannot perform online reprocessing, DT was estimated at the BOL using Eq. (3)

$$DT = M_0/(BG \cdot F \cdot C) \qquad (3)$$

where $M_0$ is the initial fissile load, BG is breeding gain (BR-1), F is annual fissile consumption rate, and C is the reactor load factor (set to 1 in this case).

For criticality calculation, KCODE card was used with 10,000 neutron histories per cycle, 2050 total cycles, and the first 50 cycles discarded. This resulted in standard deviation of $\pm$ 14 pcm. KOPTS card was activated for kinetic parameter calculations, comprising of $\beta_{eff}$ and mean neutron generating time ($\Lambda$). These parameters are important in determining reactor dynamics, especially related to the operational safety.

## RESULTS AND DISCUSSION

Table 3 summarized the $k_{eff}$ values of PCMSR using various design modifications. The values are well below $\beta_{eff}$ of each variation. With similar $k_{eff}$, it is expected that the criticality-dependent neutronic parameters can be compared fairly.

**Table 3.** $k_{eff}$ and $\beta_{eff}$ of PCMSR.

| Variation | $k_{eff}$ | $\beta_{eff}$ |
|---|---|---|
| Standard | $1.0012 \pm 0.00014$ | $0.00324 \pm 0.00016$ |
| IC-OC | $1.00224 \pm 0.00014$ | $0.00299 \pm 0.00016$ |
| IG-OC | $1.00189 \pm 0.00014$ | $0.00298 \pm 0.00016$ |
| IC-OB | $1.00167 \pm 0.00015$ | $0.00311 \pm 0.00018$ |
| IG-OB | $1.00189 \pm 0.00014$ | $0.00302 \pm 0.00017$ |
| IC-OG | $1.00218 \pm 0.00014$ | $0.00337 \pm 0.00018$ |

Kinetic parameters are depicted in Fig. 4. $\beta_{eff}$ is represented by blue bars and $\Lambda$ is shown as red line. Considering the standard deviation, there is no discernible pattern on $\beta_{eff}$ in regard to the fuel salt layer configuration. This implies that fuel salt layer addition has no direct consequences to the $\beta_{eff}$. The values are typical of reactors fueled with U-233, with the largest $\beta_{eff}$ is only around half of $\beta$ value of U-235 (0.0065) [41]. Along with the fact that the actual $\beta_{eff}$ is lower due to precursor drift, the reactivity control in PCMSR can pose different challenge that that of light water reactors (LWRs).

Meanwhile, $\Lambda$ value becomes shorter with the addition of fuel layers. The shortest is IC-OB variation, followed by IC-OC. Both variations added two fuel layers, increasing salt volume and subsequently increasing the probability of neutron interacting with the fuel. For one fuel layer addition, IG-OC has longer $\Lambda$ than IC-OG, despite both similarly added one Core channel layer. This is caused by the graphite layer in the former is located in the inner layer, giving slightly longer time for the neutron to roam and interacting with the moderator. Despite $\Lambda$ in IC-OB is almost halved from the Standard design, it is nonetheless comparable to high temperature reactor (HTR) [42] and longer than LWR [43].
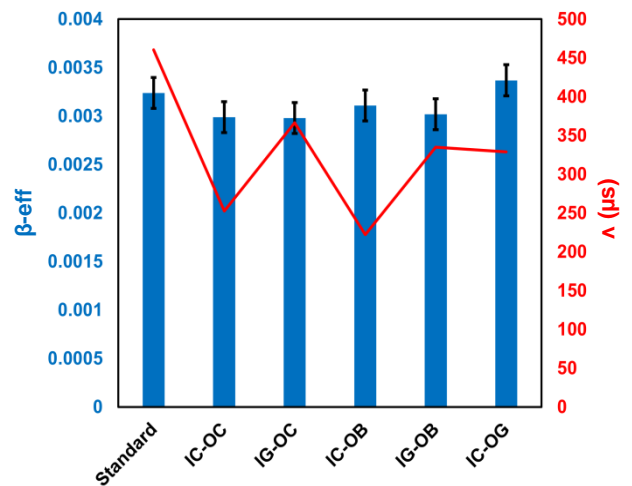


**Fig. 4.** Kinetic parameters of PCMSR with various design modifications.

Neutron spectra are displayed in Fig. 5. The spectrum is softest in Standard design, since its graphite volume is the largest, ensuring better moderation. IC-OG and IG-OC spectra are almost not discernible to each other, whilst IC-OB has the hardest spectrum as it has the smallest graphite volume.
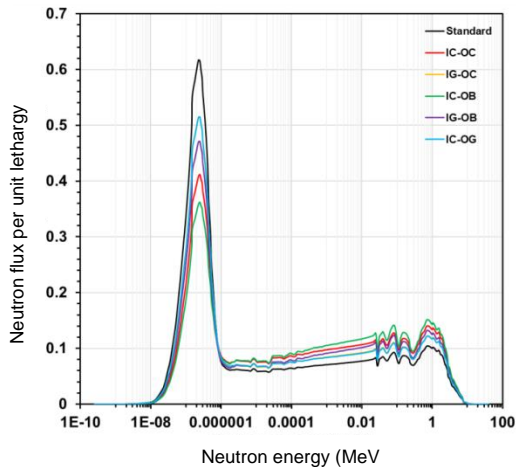


**Fig. 5.** Neutron spectra of PCMSR with various configurations.

TCR is the most important safety parameter of an MSR. Usually, MSR fueled with U-233 has weakly negative TCR, mostly as an effect of positive moderator feedback due to spectral shift of graphite in low energy region (0.2 eV) [44]. The summary of TCR values is shown in Fig. 6.
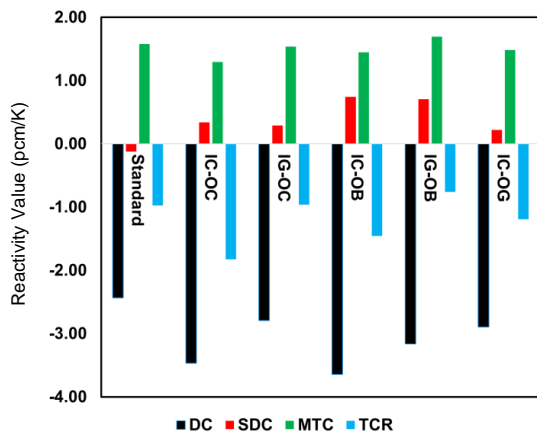


**Fig. 6.** TCR of PCMSR with various configurations.

The most apparent change is seen in DC and SDC. DC values are improved, i.e., becoming more negative as fuel layers are added. The most negative DC is in IC-OB, followed closely by IC-OC. Two additional layers provide larger fuel inventory than one additional layer, increasing negative temperature feedback from Doppler broadening. Weakest DC improvement is shown in IG-OC, as Doppler effect in outer side of the core is weaker than in the center of the core, which is why IC-OG has slightly better DC improvement than the former due to additional layer was placed in the inner layer.

Other significant change occurs in SDC. Whilst SDC in Standard design is very weakly negative, in other variations, the values are positive especially for Outer Blanket variations. Positive SDC implies that the core is in under-moderated condition which, in term of inherent safety, is not ideal for MSR [45]. In under-moderated core, partial fuel ejection from the salt expansion increases the moderator-to-fuel ratio (MFR), subsequently increasing fission reaction. Blanket layer addition shifted the moderation zone into under-moderated farther than core due to large moderator reduction, and even worse in IC-OB with the additional Core layer.

Meanwhile, MTC do not show a strong correlation to the addition of fuel layers. Although MTC is weakly improved in IC-OC and IC-OB, it is slightly worsened in IG-OB. Therefore, MTC is not a strong factor of fuel layer addition.

In total, IC-OC has the strongest negative TCR. Despite slight weakening in SDC, improved DC and MTC ensures that it has stronger negative temperature feedback than Standard design. IC-OB follows behind, lagging in more positive SDC but nevertheless improved total TCR than Standard. Meanwhile, Inner Graphite variations, IG-OC and IG-OB, both have weaker TCR than Standard, owing primarily to weakened SDC and, in the latter case, weaker MTC. In term of inherent safety, therefore, IG-OC and IG-OB variations are not preferred.

In comparison with other MSR designs, PCMSR with IC-OC variation has weaker temperature feedback coefficient (-1.83 pcm/K) than SD-TMSR (-2 pcm/K) [17] but slightly stronger than MSBR (-1.64 pcm/K) [46]. Thereby, TCR of PCMSR IC-OC is comparable with other thermal breeder MSR designs.

BR and DT are shown in Fig. 7, the former is shown as red line and the latter is in blue columns. As BR in Standard design is below unity, the DT is negative. Meaning, apart from being impossible to generate enough U-233 to start a new PCMSR, the total external fissile requirement in those 47 years is the same with its initial fissile inventory.
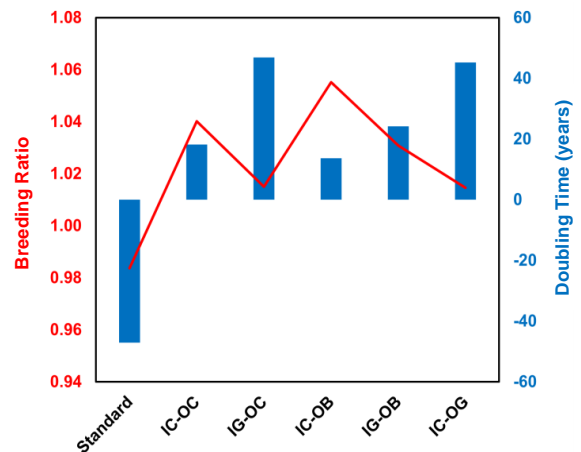


**Fig. 7.** BR and DT of PCMSR with various configurations.

All design modifications show BR above unity, fulfilling the criterion as breeder reactor. BR is the largest in IC-OB and smallest in IC-OG. This values directly correlated to the fuel salt volume, as the most fuel channel addition resulted in largest BR and the fewest addition improves only slightly above break even. Likewise, the DT is shortest in IC-OB, needing only 13.67 years to accumulate enough U-233 to start a new PCMSR. In comparison, DT of SD-TMSR is 16 years in one study [17] and 26 years in another [47], MSBR is 21 years [4], and heavy water-moderated MSR (HWMSR) is 12 years [48]. According to Eq. 3, DT is a factor of initial fissile inventory, but since its difference is not particularly significant to each other (see Table 3), BR is the strongest factor to determine DT. From this observation, IC-OB is the most preferable option in term of BR and DT.

It must be noted that the DT shown in Fig. 7 is only an estimation at the BOL. If we consider online fuel reprocessing and nuclide evolution throughout the burnup, the BR will not be constant with tendency of decreasing, and thereby DT will take longer than initially estimated. It is shown in both SD-TMSR analyses [17,47] and HWMSR [48] where the initial BR decreases at the end of life (EOL) due to the accumulation of TRUs. This must be investigated in future works with a proper calculation tool.

Table 4 summarizes PCMSR fuel inventory, with the salt proportion inside and outside the core is 1:1. Standard design requires the largest U-233 inventory, despite having the least fuel channel, due to larger Th-232 inventory than other variations. Since IC-OB was given the most amount of fuel channel addition, its initial fissile inventory is the second largest to Standard. Nevertheless, the fissile load is lower than Standard anyway, thus it is reasonably acceptable. Other variations have lower fissile inventories, but do not differ in a significant amount.

**Table 4.** Fuel inventory of PCMSR with various configurations.

| Variation | U-233 Inventory (kg) | Th-232 Inventory (kg) |
|---|---|---|
| Standard | 324.8 | 19,524 |
| IC-OC | 308.4 | 18,592 |
| IG-OC | 297.4 | 17,660 |
| IC-OB | 319.2 | 18,278 |
| IG-OB | 315.6 | 17,636 |
| IC-OG | 278.8 | 17,028 |

To provide better perspective, the initial fuel inventory of PCMSR with IC-OB variation is compared to other MSR designs, normalized to 1,000 MWe. The comparison is shown in Table 5.

**Table 5.** Initial fuel inventories of various MSR designs.

| Reactor | Initial U-233 inventory (t) |
|---|---|
| PCMSR (IC-OB) | 1.276 |
| PCMSR (Standard) | 1.388 |
| MSBR [5] | 1.304 |
| SD-TMSR [17] | 1.27 |
| SD-TMSR [47] | 1.3 |
| MSR FUJI-U3-(0) [9] | 5.665 |

Compared to MSBR and SD-TMSR, PCMSR IC-OB has similar initial fissile inventory, slightly below 1.3 tons per GWe. This is important as startup fuel requirement is non-linear to power rate, but instead depends on the buckling geometry and buckling material of the reactor. By maintaining a comparably similar initial fuel inventory when normalized to 1,000 MWe, PCMSR can minimize the upfront fuel requirement. This is beneficial when PCMSR is installed as a single or twin module, so that smaller power rate does not stretch the fissile availability.

Meanwhile, compared to MSR FUJI-U3-(0), its 200 MWe design already requires significantly larger inventory in the primary loop than a single PCMSR core module. FUJI was not intended to breed a large surplus of U-233, not equipped with online fuel reprocessing system, and designed with low power density. As a consequence, a significantly larger initial fuel inventory is required to maintain criticality for a certain period of time prior to online refueling. PCMSR, on the other hand, is operated with low excess reactivity and refueled within a significantly shorter period of time. The graphite moderator is replaced periodically, so there is no necessity to maintain a low power density. Therefore, initial PCMSR inventory can be kept minimal, much lower than MSR FUJI-U3.

## CONCLUSION

Standard PCMSR design was modified by adding Core and Blanket fuel channels in its radial graphite layers in five different variations, in order to fulfil the criteria of a breeder reactor whilst maintaining acceptable TCR and reasonable fuel inventory. From the neutronic standpoint, all modification variations fulfil BR value above unity. IC-OC variation exhibits the most negative TCR, whilst IC-OB has the largest BR and shortest DT. Normalized to 1,000 MWe nominal power, initial fuel inventory in IC-OB is still comparable to other thermal breeder MSRs. Since IC-OB also has its TCR improved as well, it has better appeal than IC-OC in case of optimal design. Therefore, IC-OB

15

variation can be applied to redesign the original PCMSR design and used in various design optimization. Future design optimizations must involve burnup calculation with considering the online reprocessing system, in order to better understand the implementation of thorium fuel cycle in PCMSR.

## ACKNOWLEDGMENT

## AUTHOR CONTRIBUTION

R. A. P. Dwijayanto conceptualize the research, perform data curation, performed the analysis, and write the manuscript. A. W. Harto provides the software, supervise the research, and performed the analysis. R. A. P. Dwijayanto is the main contributor of this article. All authors read and approved the final version of the manuscript.

## REFERENCES

1. J. Serp, M. Allibert, O. Beneš *et al.,* Prog. Nucl. Energy **77** (2014) 308.

2. J. Křepel, B. Hombourger, C. Fiorina *et al.,* Ann. Nucl. Energy **64** (2014) 380.

3. D. LeBlanc, Nucl. Eng. Des. **240** (2010) 1644.

4. E. S. Bettis, R. C. Robertson, Nucl. Applications Technol. **8** (1970) 190.

5. R. C. Robertson, Conceptual Design Study of A Single-Fluid Molten Salt Breeder Reactor (1971).

6. J. Park, Y. Jeong, H. C. Lee *et al.*, Int. J. Energy Res. **39** (2015) 1673.

7. C. Y. Zou, X. Z. Cai, D. Z. Jiang *et al.,* Nucl. Eng. Des. **281** (2015) 114.

8. B. Hombourger, J. Křepel, A. Pautz, Ann. Nucl. Energy **144** (2020) 107504.

9. S. Q. Jaradat, A. B. Alajo, Nucl. Eng. Des. **314** (2017) 251.

10. E. D. Greaves, K. Furukawa, L. Sajo-Bohus *et al.,* AIP Conf. Proc. **1423** (2012) 453.

11. K. Furukawa, L. Berrin Erbay, A. Aykol, Energy Convers. Manag. **63** (2012) 51.

12. K. Furukawa, K. Arakawa, L.B. Erbay *et al.,* Energy Convers. Manag. **49** (2008) 1832.

13. C. Yu, X. Li, X. Cai *et al.,* Ann. Nucl. Energy **85** (2015) 597.

14. C. Yu, X. Li, X. Cai *et al.,* Ann. Nucl. Energy **99** (2017) 335.

15. Y. Peng, G. Zhu, Y. Zou *et al.,* Int. J. Energy Res. (2020) 1.

16. X. X. Li, X. Z. Cai, D. Z. Jiang *et al.,* Prog. Nucl. Energy **78** (2015) 285.

17. G. C. Li, P. Cong, C. G. Yu *et al.,* Prog. Nucl. Energy **108** (2018) 144.

18. K. F. Ma, C. G. Yu, X. Z. Cai *et al.,* Nucl. Sci. Tech. **31** (2020) 1.

19. A. W. Harto, AIP Conf. Proc. **1448** (2012) 82.

20. A. W. Harto, ARPN J. Eng. Appl. Sci. **11** (2016) 3993.

21. A. W. Harto, Indones. J. Phys. Nucl. Appl. **3** (2018) 7.

22. A. W. Harto, Int. J. Nucl. Energy Sci. Technol. **9** (2015) 224.

23. R. A. P. Dwijayanto, M. R. Oktavian, M.Y.A. Putra *et al.*, A.W. Harto, Atom Indones. **47** (2021) 191.

24. N. M. K. Putri, B. JS and S. Aritonang, Int. J. Educ. Soc. Sci. Res. **5** (2022) 235.

25. T. M. Sembiring, J. Susilo and S. Pinem, J. Phys. Conf. Ser. **962** (2018) 012030.

26. M. H. du Toit and V. V. Naicker, Nucl. Eng. Des. **337** (2018) 394.

27. Zuhair, Suwoto, T. Setiadipura *et al.,* Nukleonika **64** (2019) 131.

28. Zuhair, R. A. P. Dwijayanto, Suwoto *et al.*, Kuwait J. Sci. **48** (2021) 1.

29. A. Wojciechowski, Prog. Nucl. Energy **106** (2018) 204.

30. B. Passons, P. Tsvetkov, Ann. Nucl. Energy **165** (2022) 108688.

31. Y. Jeong, J. Park, H. C. Lee *et al.,* J. Nucl. Sci. Technol. **53** (2016) 529.

32. C. A. M. da Silva, A. L. Vieira, I. R. Magalhães *et al.,* Braz. J. Radiat. Sci. **9** (2021) 1.

33. A. Khakim, F. Rhoma, A. Waluyo *et al.,* AIP Conf. Proc. **2374** (2021) 020028.

34. F. R. L. Manik, Suharyana, F. Anwar *et al.,* J. Phys. Conf. Ser. **1912** (2021) 012010.

35. A. Khakim, F. R. Firmanda, Y. Pramono *et al.,* Atom Indones. **48** (2022) 1.

36. J. P. Carter and R. A. Borrelli, Nucl. Eng. Des. **365** (2020) 110718.

37. T. Fei, B. Feng and F. Heidet, Ann. Nucl. Energy **140** (2020) 107099.

38. S. Zhou, W. S. Yang, T. Park *et al.,* Ann. Nucl. Energy **114** (2018) 369.

39. J. Shi and M. Fratoni, EPJ Web Conf. **247** (2021) 06040.

40. D. Moser, A. Wheeler and O. Chvála, Ann. Nucl. Energy **110** (2017) 1.

41. J. R. Lamarsh, Introduction to Nuclear Reactor Theory, Addison-Wesley Publishing, Boston (1966).

42. Zuhair, Suwoto, T. Setiadipura *et al.,* Acta Polytech. **60** (2020) 175.

43. D. Hartanto, A. Alshamsi, A. Alsuwaidi *et al.,* Atom Indones. **46** (2020) 177.

44. L. Mathieu, D. Heuer, R. Brissot *et al.,* C. Garzenne Prog. Nucl. Energy **48** (2006) 664.

45. G. Zhu, Y. Zou, R. Yan *et al.,* Int. J. Energy Res. **43** (2019) 577.

46. A. Rykhlevskii, J. W. Bae and K. D. Huff, Ann. Nucl. Energy **128** (2019) 366.

47. O. Ashraf, A. Rykhlevskii, G. V. Tikhomirov *et al.,* Ann. Nucl. Energy **137** (2020) 107115.

48. J. Wu, J. Chen, X. Kang *et al.,* Ann. Nucl. Energy **132** (2019) 391.